Check for updates

Received: 16 April 2022 | Revised: 7 September 2022 | Accepted: 8 September 2022

DOI: 10.1002/asl.1131

RESEARCH ARTICLE

Atmospheric Science Letters RMetS

# Primary characteristics of the extreme heavy rainfall event over Henan in July 2021

**Jianhua Sun**[1,2,3] | **Shenming Fu**[4] | **Huijie Wang**[1] | **Yuanchun Zhang**[1] | **Yun Chen**[5] | **Aifang Su**[6] | **Yaqiang Wang**[7] | **Huan Tang**[1] | **Ruoyun Ma**[1]

[1]Key Laboratory of Cloud-Precipitation Physics and Severe Storms (LACS), Institute of Atmospheric Physics, Chinese Academy of Sciences (IAP/CAS), Beijing, China

[2]State Key Laboratory of Severe Weather, Chinese Academy of Meteorological Sciences, Beijing, China

[3]Southern Marine Science and Engineering Guangdong Laboratory (Zhuhai), Zhuhai, China

[4]International Center for Climate and Environment Sciences (ICCES), Institute of Atmospheric Physics, Chinese Academy of Sciences (IAP/CAS), Beijing, China

[5]National Meteorological Center (NMC), China Meteorological Administration (CMA), Beijing, China

[6]Henan Meteorological Observatory, Zhengzhou, China

[7]Institute of Artificial Intelligence for Meteorology, Chinese Academy of Meteorological Sciences (CAMS), Beijing, China

**Correspondence**
Jianhua Sun, Key Laboratory of Cloud-Precipitation Physics and Severe Storms (LACS), Institute of Atmospheric Physics, Chinese Academy of Sciences (IAP/CAS), Beijing 100029, China.
Email: sjh@mail.iap.ac.cn

Shenming Fu, International Center for Climate and Environment Sciences (ICCES) International Center for Climate and Environment Sciences (ICCES), Institute of Atmospheric Physics, Chinese Academy of Sciences (IAP/CAS), Beijing 100029, China.
Email: fusm@mail.iap.ac.cn

**Funding information**
The National Key Research and Development Program of China, Grant/Award Number: 2019YFC1510400; The National Natural Science Foundation of China, Grant/Award Numbers: 42075002, 41975057, U2142202

## Abstract

During mid-July 2021, an extreme heavy rainfall event (HRE) occurred in Henan Province (hereafter “21.7” HRE), with extreme hourly precipitation of 201.9 mm appearing at Zhengzhou station. Our preliminary analyses of the “21.7” HRE using the observations and ECMWF (European Centre for Medium-Range Weather Forecasts) ERA5 reanalysis data, reached the following conclusions. Favorable configurations of various synoptic weather systems (e.g., strong upper-level high-pressure ridge, intense middle-level low-pressure trough) acted as crucial background conditions for the occurrence of the “21.7” HRE. A 21-h long-lived mesoscale convective vortex (MCV), mainly located in the middle and lower troposphere west of Zhengzhou city, was a key system that produced the extreme hourly rainfall of 201.9 $mm{\cdot}h^{-1}$. The MCV's development/sustainment was dominated by the vertical transport of cyclonic vorticity and tilting, as well as the horizontal import of cyclonic vorticity to the vortex's key region. In contrast, the divergence-related vertical shrinking was the most detrimental factor. Lagrangian moisture transport analysis showed that moisture for the extreme heavy rainfall in Zhengzhou on July 20 mainly came from levels below 2200 m, driven by airflows on the peripheries of tropical cyclones IN-FA and CEMPAKA. To enhance the understanding of “21.7” HRE, we suggest more in-depth investigations in the future.

This is an open access article under the terms of the Creative Commons Attribution License, which permits use, distribution and reproduction in any medium, provided the original work is properly cited.
© 2022 The Authors. *Atmospheric Science Letters* published by John Wiley & Sons Ltd on behalf of the Royal Meteorological Society.



1530261x, 0, Downloaded from https://rmets.onlinelibrary.wiley.com/doi/10.1002/asl.1131 by Institution Of Atmospheric Physics, Wiley Online Library on [29/11/2022]. See the Terms and Conditions (https://onlinelibrary.wiley.com/terms-and-conditions) on Wiley Online Library for rules of use; OA articles are governed by the applicable Creative Commons License

# 1 | INTRODUCTION

During 17 to 22 July, 2021, an extreme heavy rainfall event (HRE) occurred in Henan Province (hereafter "21.7" HRE). As released by the government of Henan Province, more than 14.78 million people across the province have been affected with 398 dead or missing, and a direct economic loss of up to ~120 billion Yuan has been caused (Fu, Tang, et al., 2022; Fu, Zhang, et al., 2022; Li et al., 2022; Yin et al., 2022).

The rainbelts in North China are one of the summer's three major rainfall regions in China (Tao, 1980). Some HREs occurred in North China since the founding of the People's Republic of China, which produced flood disasters. For examples, the HRE in July 1958 in the middle reaches of the Yellow River Basin ("58.7" HRE), the HRE in August 1963 in Hebei Province ("63.8" HRE), the "75.8" HRE in August 1975 in Henan Province ("75.8" HRE), and the HRE in August 1996 in Hebei Province ("96.8" HRE). All of these events brought huge disaster. Among these events, "75.8" HRE, an extreme HRE in the south of Henan province during 5 to 7 August 1975, caused the biggest meteorological disaster after the founding of the people's Republic of China, which brought a catastrophic flooding that killed tens of thousands of people. Chinese researchers have studied the large-scale circulation conditions and related mesoscale convection that produced extreme heavy rainfall during this event (Ding, 2015; Tao, 1980). Luo et al. (2020) have reviewed the advanced studies on heavy rainfall in North China. The characteristics of heavy rainfall in North China have been revealed more clearly and quantitatively by using intensive observation data with high temporal and spatial resolution.

HREs in North China are often accompanied by severe convection with intense short-duration heavy rainfall (hourly precipitation ≥20 mm) (Luo et al., 2016; Sun et al., 2013; Zhang & Zhai, 2011). Some previous studies have demonstrated the major synoptic weather patterns associated with heavy rainfall in North China (Compilers of Heavy rainfall in North China, 1992; Ding et al., 1980; Sun et al., 2005). Heavy rainfall in North China mainly occurs under the circulation pattern featuring a high-pressure system to the East and a low-pressure system to the West. The vortex, warm shear line, trough, cold front, and low-level jet are the main synoptic scale systems causing heavy rainfall in North China. Most severe heavy rainfall events in North China occur under the interaction of two or more aforementioned synoptic systems. In addition, because of the complex terrain in North China, the terrain and underlying surface also impact on the triggering and maintenance of convection. Under stable synoptic weather patterns, the terrain and urban thermal processes have a noticeable increasing effect on the intensity of rainfall (Sun & Yang, 2008; Xia & Zhang, 2019), and the mesoscale rainstorms mainly occur around the evening and early morning (Sun, 2005; Sun & Yang, 2008).

Although many studies have been carried out on the synoptic scale conditions, topographic effects, and the triggering and development process of the mesoscale convective system for the formation of heavy rainfall in North China, the formation mechanism of "21.7" HRE is not fully understood. Therefore, more in-depth studies are needed to reveal further the complicated mechanisms of this "21.7" HRE in Henan Province. This article only attempts to briefly introduce the observations and answer the following two questions from an academic viewpoint: (1) What were the synoptic and mesoscale weather systems associated with the HRE on July 20, 2021? (2) How was moisture transported to Henan Province and where were the source regions of the moisture?

# 2 | DATA AND METHOD

Hourly precipitation observations and three-hourly surface observations from China Meteorological Administration were used to analyze the rainfall variation characteristics of "21.7" HRE in Henan Province and the surface weather systems. The hourly 0.25° × 0.25° European Centre for Medium-Range Weather Forecasts (ECMWF) ERA5 data (Hersbach et al., 2020) was employed to diagnose the evolution of mesoscale convective vortex (MCV) and also used as input fields that drove the moisture trajectories' calculation.

As the vorticity budget was an effective method to investigate the evolution of a vortex (Fu et al., 2017, 2019), we used the following vorticity budget equation:

$$\frac{\partial\zeta}{\partial t} = \underbrace{-\boldsymbol{V}_{\mathrm{h}}\cdot\nabla_{\mathrm{h}}\zeta}_{\text{HAV}} \underbrace{-\,\omega\frac{\partial\zeta}{\partial p}}_{\text{VAV}} \underbrace{-\,\boldsymbol{k}\cdot\left(\frac{\partial\boldsymbol{V}_{\mathrm{h}}}{\partial p}\times\nabla_{\mathrm{h}}\omega\right)}_{\text{TIL}} \underbrace{-\,\beta v}_{\text{PVA}} \underbrace{-\,(\zeta+f)\nabla_{\mathrm{h}}\cdot\boldsymbol{V}_{\mathrm{h}}}_{\text{STR}} \tag{1}$$

where ($\boldsymbol{i}, \boldsymbol{j}, \boldsymbol{k}$) are the unit vectors in the east, north, and zenith direction, respectively; $\zeta$ is relative vorticity in the $\boldsymbol{k}$ direction, $\boldsymbol{V}_{\mathrm{h}} = u\boldsymbol{i} + v\boldsymbol{j}$ denotes horizontal wind, $\nabla_{\mathrm{h}} = \frac{\partial}{\partial x}\boldsymbol{i} + \frac{\partial}{\partial y}\boldsymbol{j}$ is horizontal gradient operator, $p$ is the pressure, $\omega$ is the vertical velocity in the pressure coordinate, $f$ is Coriolis parameter, and $\beta = \frac{\partial f}{\partial y}$. HAV and VAV are horizontal and vertical advections of vorticity, respectively. Terms TIL, PVA, and STR are tilting, planetary vorticity advection, and stretching, respectively. The sum

1530261x, 0, Downloaded from https://rmets.onlinelibrary.wiley.com/doi/10.1002/asl.1131 by Institution Of Atmospheric Physics, Wiley Online Library on [29/11/2022]. See the Terms and Conditions (https://onlinelibrary.wiley.com/terms-and-conditions) on Wiley Online Library for rules of use; OA articles are governed by the applicable Creative Commons License

of HAV, VAV, TIL, PVA, and STR was defined as the total effect term (TOT).

The Hybrid Single-Particle Lagrangian Integrated Trajectory (HYSPLIT) model (Draxler & Hess, 1998; Stein et al., 2015) was used to calculate 96 h back trajectories for air parcels at three critical levels (500, 1500, and 3000 m) over Henan Province. To understand the major features of trajectories, the cluster technique based on the total spatial variance method (Draxler, 1999) was used, then the total moisture supply contribution was calculated as

$$Q_{all} = \left( \sum_{1}^{m} \sum_{it=1}^{96} q_{it} / \sum_{1}^{n} \sum_{it=1}^{96} q_{it} \right) \times 100\% \quad (2)$$

where $m$ is the number of trajectories in each cluster, $n$ is the total number of trajectories in all clusters, and $q_{it}$ is the specific humidity of the air parcel at each time step along each trajectory.

# 3 | OVERVIEW

## 3.1 | The observed precipitation

From 17 to 22 July, 2021, Henan Province suffered from an extreme HRE that lasted 6 days. The main characteristics of the HRE were that the accumulated rainfall was substantial and the short-duration heavy rainfall was extreme. The accumulated precipitation exceeded 500 mm in large areas of central and northern Henan Province (Figure 1a) with the strongest rainfall centers mainly appearing in Zhengzhou, Hebi, Xinxiang, and Anyang cities. The accumulated precipitation in northern Henan Province was more than half of the annual precipitation in 30 years (1989–2018) (Figure 1b). The accumulated precipitation in two national weather stations (Zhengzhou and Anyang) exceeded their respective annual precipitation (Figure 1b). The 6-day accumulated precipitation at Baizhai station in Zhengzhou city and

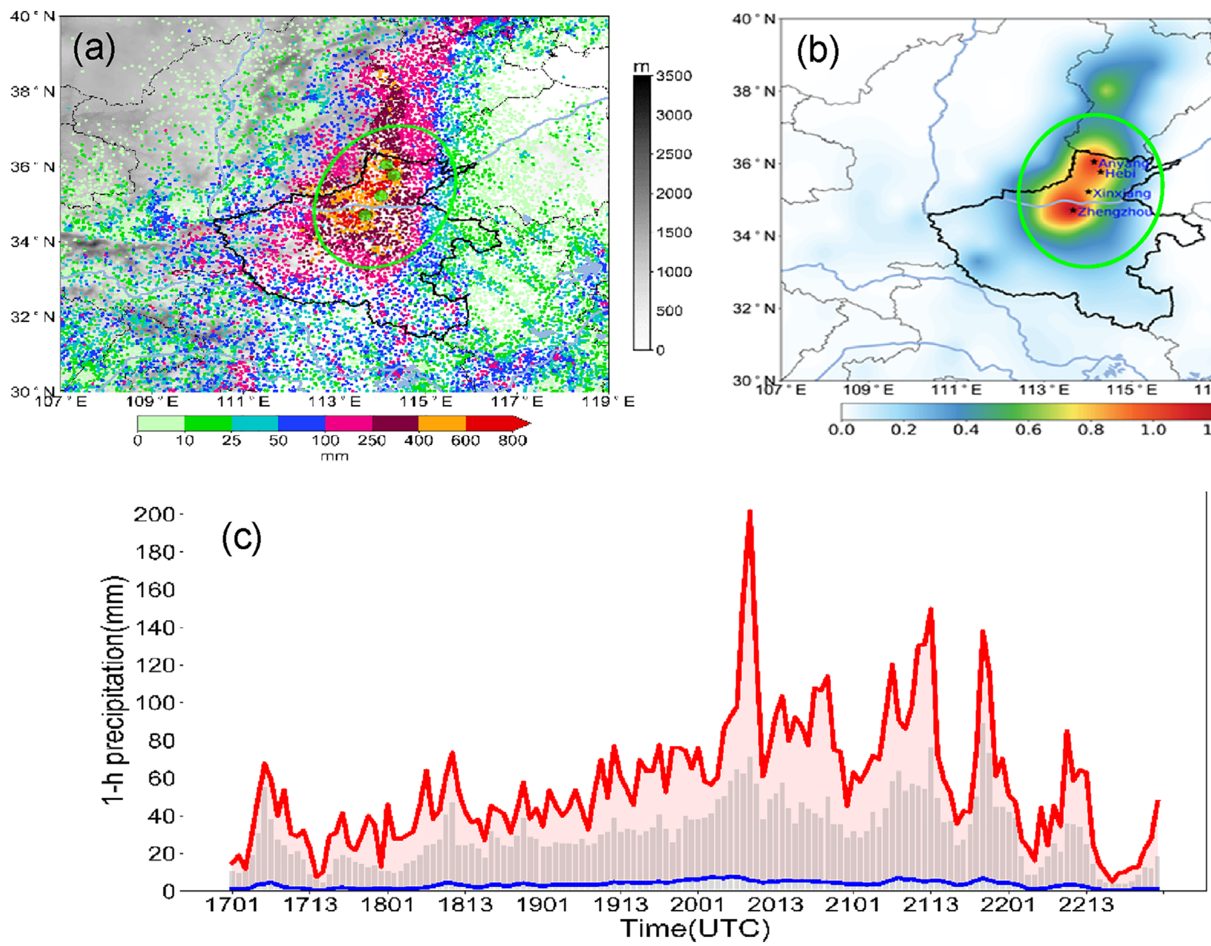


FIGURE 1 (a) The accumulated precipitation of automatic weather stations from 0000 UTC 17 to 0000 UTC 24 July, 2021, where the shading is the terrain. (b) The ratio of 6-day cumulative precipitation of national weather stations to average annual precipitation from 1989 to 2018. The four dots in (a) and (b) represent Zhengzhou, Xinxiang, Hebi, and Anyang stations, respectively. (c) Variation of hourly precipitation at automatic weather stations in Henan Province from 0000 UTC 17 to 2000 UTC 24 July, 2021. The red and blue lines represent the maximum value and average value, respectively. The gray bar shows the 99th quantiles of all stations in each hour. The precipitation data is provided by National Meteorological Center, China Meteorological Administration, and the date format is ddhh (UTC).

1530261x, 0, Downloaded from https://rmets.onlinelibrary.wiley.com/doi/10.1002/asl.1131 by Institution Of Atmospheric Physics, Wiley Online Library on [29/11/2022]. See the Terms and Conditions (https://onlinelibrary.wiley.com/terms-and-conditions) on Wiley Online Library for rules of use; OA articles are governed by the applicable Creative Commons License

Kechuang center station in Hebi city exceeded 993.1 and 1122.6 mm, respectively. The hourly precipitation of 201.9 mm·h$^{-1}$ occurred at 0800–0900 UTC, on 20 July at Zhengzhou station (Figure 1c), which was the maximum hourly precipitation since the establishment of this station in 1951. Several stations observed heavy rainfall with hourly precipitation of more than 100 mm·h$^{-1}$, and the differences between the hourly maximum precipitation and the 99th quantile value at most times were more than 50 mm from 20 to 21 July, which indicated inhomogeneity of this precipitation event.

## 3.2 | Synoptic analyses

During "21.7" HRE, the South Asia high (SAH) was strong (Figures 2a,b), with its center mainly located over the western section of the Tibetan Plateau. An upper-level jet was maintained around the northern periphery of the high, east of which the jet broken into two branches, resulted in strong upper-level divergence northeast of the SAH. To the east of the SAH, there was an upper-level shortwave through within the band of 100°–110° E (Figures 2a,b), a strong high-pressure ridge within the band of 110°–120° E, and another shortwave through within the band of 120°–130° E. Of these, Henan Province was governed by the strong high-pressure ridge, which was associated with an intense upper-level divergence. This acted as a favorable condition for ascending motions and heavy rainfall.

In the middle troposphere, as shown in Figures 2c,d, a shortwave trough appeared over the Tibetan Plateau. The isohypses were sparse in the east of the trough and the wind was weak within the band of 100°–105°E. East of this, a low-pressure trough was maintained over Henan Province, where a strong warm advection appeared. The warm advection contributed to enhancing ascending motions (Holton, 2004) and lowering the

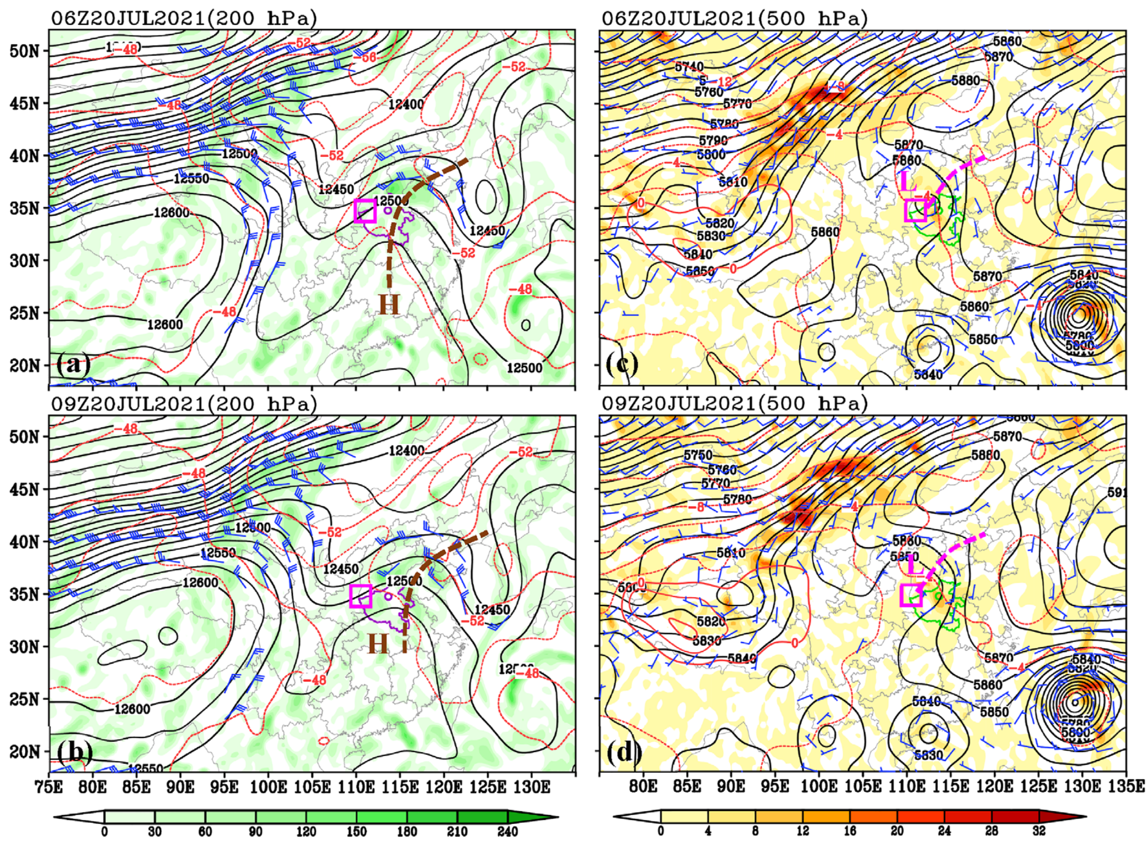


FIGURE 2 (a,b) Show the divergence (shading, $10^{-6} \cdot s^{-1}$), geopotential height (black contour; gpm), wind above 25 ms$^{-1}$ (a full bar is 10 m · s$^{-1}$) and temperature (red contours; °C) at 200 hPa, where the thick brown dashed lines are the ridge lines, and "H" mark the high-pressure ridge. Panels (c, d) show the temperature advection (shading, $10^{-5}$ K · s$^{-1}$), geopotential height (black contour; gpm), wind above 5 m · s$^{-1}$ (a full bar is 10 m · s$^{-1}$) and temperature (red contours; °C) at 500 hPa, where the thick purple dashed lines are the trough lines, and "L" mark the low-pressure trough. The purple boxes outline the key region of the mesoscale convective vortex, and the small purple circle mark the location of Zhengzhou.

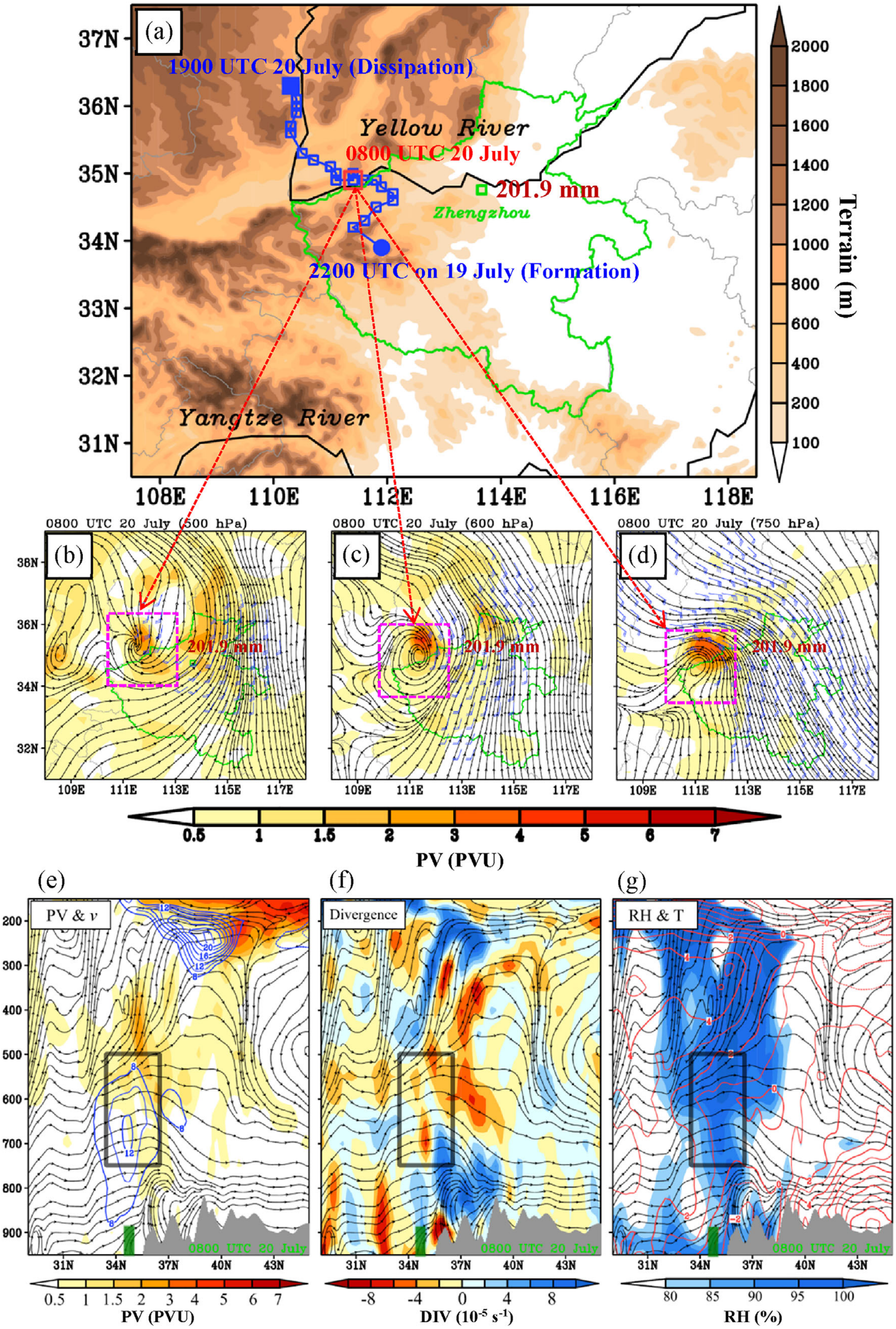


FIGURE 3 Legend on next page.

1530261x, 0, Downloaded from https://rmets.onlinelibrary.wiley.com/doi/10.1002/asl.1131 by Institution Of Atmospheric Physics, Wiley Online Library on [29/11/2022]. See the Terms and Conditions (https://onlinelibrary.wiley.com/terms-and-conditions) on Wiley Online Library for rules of use; OA articles are governed by the applicable Creative Commons License

low-level pressure (Markowski & Richardson, 2010), both of which were favorable for the "21.7" HRE. The subtropical high at 500 hPa was located a great distance north of its climatic mean (not shown). Its center was located around the Sea of Japan and merged with the continental high pressure, forming a stable "high pressure dam" in the area from Northeast China to Japan (Figures 2c,d). This is a favorable condition for the sustainment of heavy rainfall. There were two typhoons to the south and southwest of the subtropic high: Typhoon IN-FA over the Western Pacific and Typhoon CEMPAKA over the South China Sea. The easterly wind with wind speed $\geq$12 m·s$^{-1}$ (low-level jet) between Typhoon IN-FA and subtropical high transported warm and moist air to Henan Province. At the same time, the easterly wind between Typhoon CEMPAKA and the western Pacific subtropical high also transported warm and humid air to Henan Province.

In the lower troposphere, the most notable feature was that there was maintained a long-lived mesoscale convective vortex (MCV; Figure 3) around Henan Province. The MCV acted as a crucial condition for the extreme hourly rainfall over Zhengzhou. As discussed above, the coexistence of upper-, middle-, and low-level systems (e.g., the upper-level high-pressure ridge, middle-level low-pressure trough, tropical cyclones, low-level jet, etc.) was highly conducive to the occurrence of "21.7" HRE in Henan Province, which was consistent with previous research results (Ding, 2015; Sun et al., 2005; Tao, 1980). However, the major heavy-rainfall-producing weather systems differed for these famous HREs (Tao, 1980). For the "75.8" HRE in Henan Province, it was mainly due to a northward moving typhoon; for the "96.8" HRE in Hebei Province, it was mainly induced by a northeastward moving southwest vortex; and for the "58.7" HRE in the middle reaches of the Yellow River Basin, the heavy precipitation was a result from the combined effects of a southwest vortex, a trough, and a cold front. In contrast, for the "21.7" HRE in this present study, the MCV was of crucial importance.

## 4 | ANALYSES ON THE MESOSCALE CONVECTIVE VORTEX

### 4.1 | Verification of the MCV

At 2200 UTC on 19 July, a vortex formed at the location shown by the blue dot (~33.9°N, 111.9°E) in Figure 3a with its center appearing at 600 hPa. It was a mesoscale convective vortex (Bartels & Maddox, 1991; Davis et al., 2004) since: (i) It had a maximum radius of ~150 km, a maximum depth of ~3.0 km (from 750 to 500 hPa, not shown) and a 22-h life span (from 2200 UTC 19 to 1900 UTC on 20 July, Figure 2a). (ii) It was mainly located within the stratiform region of the heavy-rain-producing mesoscale convective system in Henan (not shown). (iii) It had a strong warm core (in terms of temperature deviation) of 4 K, which was located around 400 hPa (not shown). (iv) Within the MCV's main body, the latent heating release was strong, as suggested by the >1 PVU (1 PVU = 10$^{-6}$ K·m$^2$·kg$^{-1}$· s$^{-1}$) potential vorticity.

### 4.2 | Relationship of the MCV with the extreme strong hourly rainfall

After formation, the MCV mainly moved northward (Figure 3a) under the strong southerly steering airflow west of the subtropical high. In the earlier stage of the vortex (2200 UTC 19–0900 UTC on 20 July), it produced strong precipitation in Henan (Figure 1c). The rainfall intensity also increased rapidly. The maximum hourly precipitation of 201.9 mm · h$^{-1}$ appeared at Zhengzhou station between 0800 and 0900 UTC on 20 July. During this period, the MCV was mainly located between 750 and 500 hPa (Figures 2e–g), around 34.9°N, 111.4°E (Figure 3a), and the Zhengzhou station was situated ~250 km east of its center (Figures 2b–d). Strong MCV-associated southerly wind ($\geq$8 m·s$^{-1}$) influenced Zhengzhou station (Figures 3b–g), which mainly appeared in layers between 875 and 525 hPa. The strong southerly

FIGURE 3 (a) Shows the track of the MCV (blue solid line with small boxes, where the closed circle and box mark the formation and dissipation locations of the vortex, respectively, and the small red box marks the location of the vortex when the maximum hourly precipitation of 201.9 mm appeared in Zhengzhou), where shading is the terrain (units: m). (b–d) Show the horizontal stream field, potential vorticity (PV; shading, units: PVU; 1 PVU = 10$^{-6}$ K·m$^2$·kg$^{-1}$·s$^{-1}$) and wind above 8 m·s$^{-1}$ (a full wind bar is 4 m·s$^{-1}$) at 500 hPa (top level of the vortex), 600 hPa (central level of the vortex), and 750 hPa (bottom level of the vortex), respectively, where purple dashed boxes mark the central regions of the MCV. (e–g) Are cross-sections along Zhengzhou (i.e., small green boxes in [a–d]), where the vertical stream fields were composited by meridional wind ($v$; m·s$^{-1}$) and vertical velocity (cm·s$^{-1}$), green bars mark the location of the maximum hourly precipitation, big thick gray boxes outline the latitude range and vertical extent of the MCV, and gray shading are the terrain. Shading and blue contours in € are PV (PVU) and meridional wind (m s$^{-1}$), respectively; shading in (f) is divergence (DIV; 10$^{-5}$·s$^{-1}$); shading and red contours in (g) are relative humidity (RH; %) and temperature deviation (TD; K), respectively.

1530261x, 0, Downloaded from https://rmets.onlinelibrary.wiley.com/doi/10.1002/asl.1131 by Institution Of Atmospheric Physics, Wiley Online Library on [29/11/2022]. See the Terms and Conditions (https://onlinelibrary.wiley.com/terms-and-conditions) on Wiley Online Library for rules of use; OA articles are governed by the applicable Creative Commons License

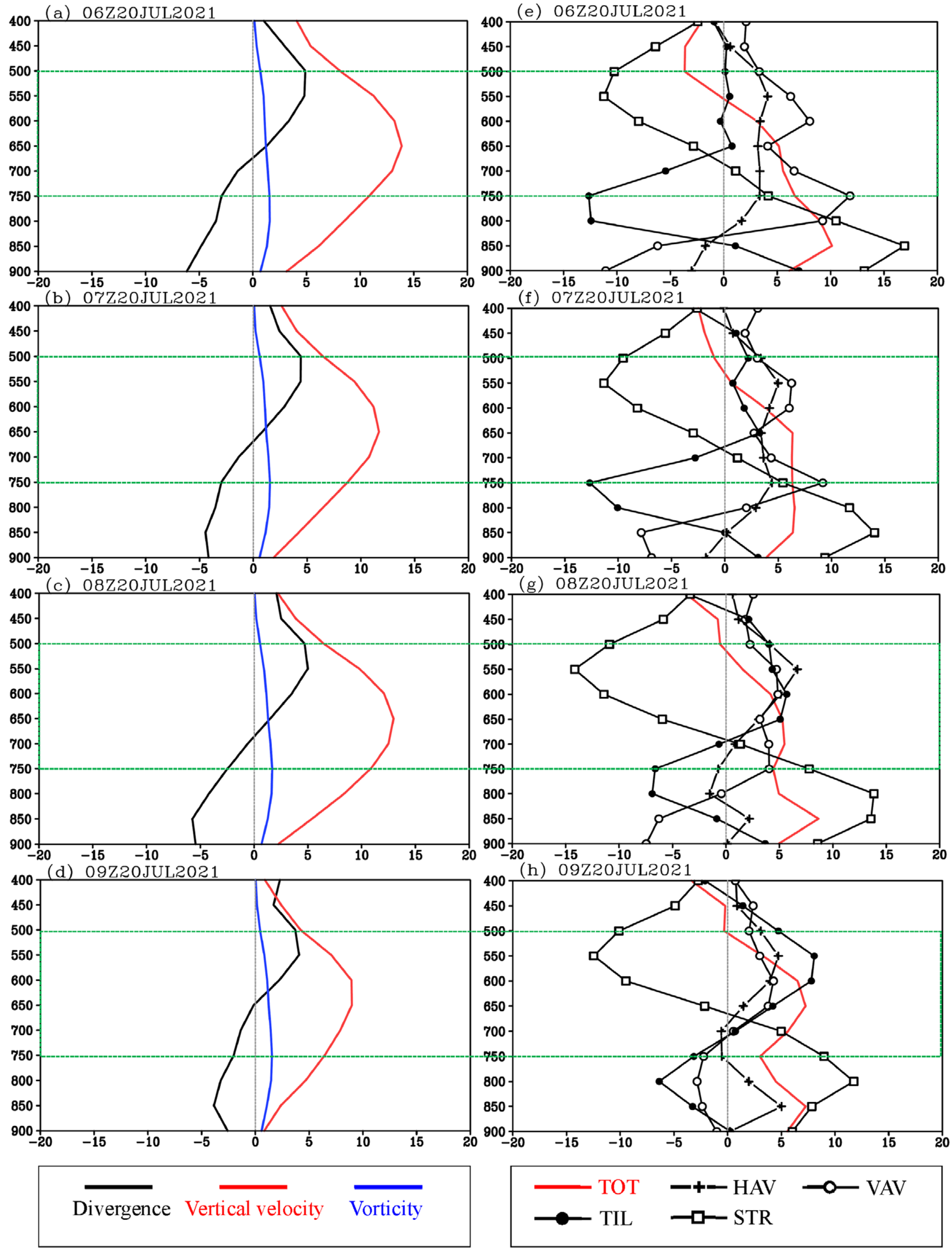


**FIGURE 4** (a–d) show the key-region averaged divergence ($10^{-5}\cdot s^{-1}$), vorticity ($10^{-4}\cdot s^{-1}$), and vertical motions ($cm\cdot s^{-1}$). (e–h) Show the key-region averaged vorticity budget terms ($10^{-9}\cdot s^{-2}$). The green dashed lines outline the vertical stretching of the mesoscale convective vortex, and the gray dashed lines mark the value of zero.

wind decelerated in the region immediately south of the mountain around 37°N (Figure 3e), mainly due to the mountain drag effect (Carissimo et al., 1988; Tutiš & Ivančan-Picek, 1991), which resulted in strong convergence within the MCV's vertical extent (Figure 3f). The strong convergence contributed to intense ascending

1530261x, 0, Downloaded from https://rmets.onlinelibrary.wiley.com/doi/10.1002/asl.1131 by Institution Of Atmospheric Physics, Wiley Online Library on [29/11/2022]. See the Terms and Conditions (https://onlinelibrary.wiley.com/terms-and-conditions) on Wiley Online Library for rules of use; OA articles are governed by the applicable Creative Commons License

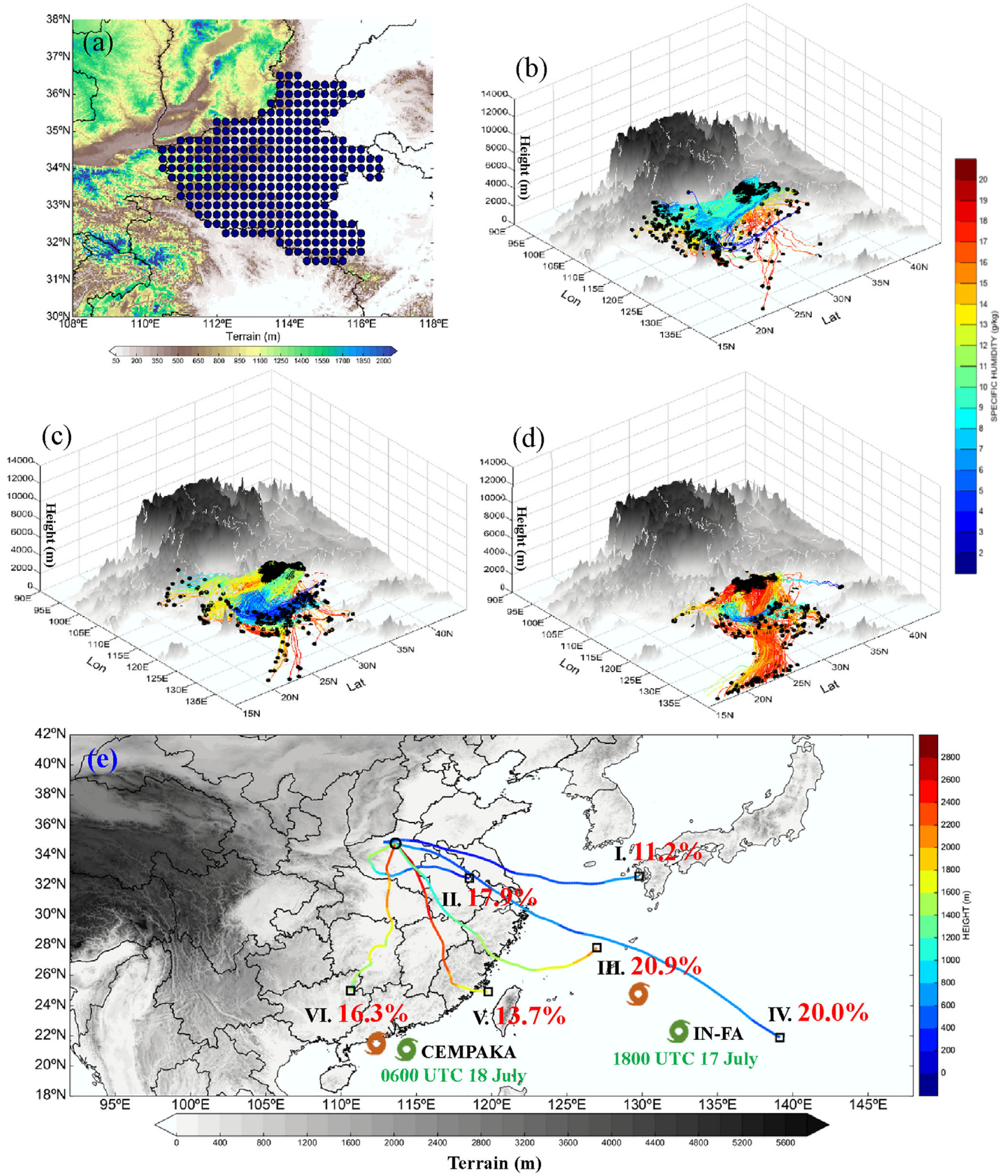


**FIGURE 5** (a) Shows the horizontal locations of the dots (blue circles) used for backward trajectory analyses, where shading is the terrain (units: m). (b–d) Show the backward trajectories ended at 3000, 1500, and 500 m, respectively, where shading represents specific humidity (units: G·kg$^{-1}$) and the black dots over Henan Province (31.5–36.5°N, 110–116°E) mark the starting locations (i.e., at 0900 UTC 20 July) for the backward trajectory analyses. (e) Shows the clustering results of backward trajectories in (b–d), where shading shows the height of air particles (units: m), small black boxes and circles mark the starting and ending locations, respectively, red values are the moisture contributions of the clustered water vapor channels, green typhoon icons show their formation locations and red icons show their locations when the maximum hourly precipitation of above 200 mm·h$^{-1}$ appeared.

1530261x, 0, Downloaded from https://rmets.onlinelibrary.wiley.com/doi/10.1002/asl.1131 by Institution Of Atmospheric Physics, Wiley Online Library on [29/11/2022]. See the Terms and Conditions (https://onlinelibrary.wiley.com/terms-and-conditions) on Wiley Online Library for rules of use; OA articles are governed by the applicable Creative Commons License

motion above the layer where the MCV located (500–300 hPa). The atmosphere was nearly saturated in this layer (Figure 3g), which was conducive to the persistence of heavy precipitation. This further favored the maintenance of intense latent heating release in the layers of 500–300 hPa, which could be reflected by the strong (∼4 K) positive temperature deviation (Figure 3g) and a PV center of ≥1.5 PVU (Figure 3e). Latent heating in turn promoted convergence and ascending motion, which formed positive feedback (Fu et al., 2017; Raymond & Jiang, 1990). This was one of the most important and direct factors that contributed to the occurrence of the extreme heavy precipitation in Zhengzhou city on July 20.

### 4.3 | Evolutionary mechanisms of the MCV

From 0600 to 0900 UTC on 20 July, within the key region of the MCV (a 2° × 2° box; Fu, Zhang, et al., 2022; Fu, Tang, et al., 2022), strong convergence dominated below 650 hPa (Figures 4a–d), and at the levels above 650 hPa, intense divergence appeared. This vertical configuration was conducive to maintaining upward motions. Meanwhile, the cyclonic vorticity and strong ascending motions dominated the key region, which favored heavy rainfall.

The vorticity budget results show that, from 0600 to 0900 UTC on 20 July, term TOT mainly were maintained a positive value in the vertical stretching of the MCV (Figures 4e–h), except for the layer of 550–500 hPa during the period from 0600 UTC to 0700 UTC on 20 July (Figures 4e.f). This means that conditions were favorable for enhancing the MCV. Comparisons among all terms showed that, from 0600 to 0700 UTC on 20 July (Figures 4e,f), the upward transport of cyclonic vorticity (i.e., VAV) was the most favorable factor for the maintenance/development of the MCV; whereas, from 0800 UTC to 0900 UTC on 20 July (Figures 4e, f), the tilting effect (i.e., TIL) enhanced rapidly and became the most favorable factor. Overall, from 0600 to 0900 UTC on 20 July, the horizontal transport (i.e., HAV) was conducive to the MCV. There was a sharp contrast between the budget results of the vortex in this study and those in previous studies (Feng et al., 2019; Fu et al., 2017, 2019; Zhang et al., 2019): the term STR was overall detrimental to the maintenance/development of the MCV in this study, whereas, in previous studies, it was the most favorable factor. The difference was because that divergence controlled the vertical stretching of the MCV in this study, and the convergence was dominant for the mesoscale vortices in previous studies.

## 5 | MOISTURE TRANSPORT ANALYSIS

A 96-h backward (i.e., from 0900 UTC on 20 to 0900 UTC 16 on July) trajectory analysis (Stein et al., 2015) was conducted using the 303 dots shown in Figure 5a. A total of 3 levels were used in the trajectory analysis: 500, 1000, and 3000 m. Overall, the trajectories sourced from the lower level over the ocean southeast of China had the largest specific humidity (Figure 5d). In contrast, the smallest specific humidity was associated with the trajectories sourced from the middle-level over South China (Figure 3b). It can be found from the trajectories shown in Figures 5b–d that, air particles mainly came from regions east, south, and southeast of Henan Province and almost no air particles originated from the regions north and northwest of Henan Province. This indicated that cold air was notably inactive in Henan province before 0900 UTC on 20 July. A cluster of the trajectories (Sun et al., 2016) is shown in Figures 3b–d resulted in 6 moisture transport channels (Figure 5e). Of these, channels IV (20% in contribution) and VI (16.3%) were mainly due to tropical cyclones IN-FA and CEMPAKA, respectively. Channels I–III and V were mainly due to interactions between two tropical cyclones and the subtropical high (an accumulated contribution of 63.7%). In addition, Channel II (17.9%) was a short transportation track that originated from east China. Comparison among the moisture transport channels showed that I, II, and IV mainly came from levels below 800 m (the accumulated contribution was 49.1%) whereas III, V, and VI mainly came from levels between 1400 and 2200 m (the accumulated contribution was 50.9%).

## 6 | SUMMARY AND DISCUSSION

In this research, the observed precipitation and large-scale circulations of the "21.7" HRE in Henan Province are first introduced, and the development of an MCV and the moisture source for the extreme heavy hourly precipitation of 201.9 mm·h$^{-1}$ over Zhengzhou during 0800–0900 UTC on 20 July are then investigated. The major large-scale circulation during this event was a typical synoptic pattern that was conducive to heavy rainfall events in North China, including strong upper-level divergence associated with a strong upper-level high-pressure ridge, intense middle-level warm advection associated with a low-pressure trough, and the vortex or shear-line in the lower troposphere. The extreme hourly heavy rainfall in Zhengzhou was closely related to a typical MCV, which was not often observed in China. Usually, heavy rainfall in China was more closely related to the meso-α-scale

1530261x, 0, Downloaded from https://rmets.onlinelibrary.wiley.com/doi/10.1002/asl.1131 by Institution Of Atmospheric Physics, Wiley Online Library on [29/11/2022]. See the Terms and Conditions (https://onlinelibrary.wiley.com/terms-and-conditions) on Wiley Online Library for rules of use; OA articles are governed by the applicable Creative Commons License

vortices such as the Tibetan Plateau vortex, southwest vortex, and Dabie vortex (Fu et al., 2020, 2021). For the MCV in this event, vorticity budget showed that, the convection-related VAV and TIL, as well as the HAV dominated the vortex's development/sustainment, whereas, the divergence-related STR was the most detrimental factor. This was notably different from the governing mechanisms of the southwest vortices (Feng et al., 2019) and Dabie vortices (Fu et al., 2017). Lagrangian moisture transport analysis showed that the moisture mainly came from the Western Pacific and the South China Sea below 2200 m, which was related to the activities of two tropical cyclones IN-FA and CEMPAKA.

Generally, the HRE took place under very favorable large-scale circulations. Therefore, it was not difficult to predict the occurrence and area of rainfall. However, this event was an extreme heavy rainfall since the "75.8" HRE in Henan Province, and the total precipitation maximum was more than 1000 mm, a rare occurrence in Henan Province and even in China. It was challenging to predict the location and intensity of the extreme or severe heavy rainfall center. Before accurately predicting the location and intensity of severe heavy rainfall, there is still a long way to go. As heavy rainfall studies mainly focus on the event in South China and the Yangtze River Basin during the past 20 years, the forecast signals for the medium-range forecast, and the triggering mechanisms of local severe convections associated with special circulations and distribution of the terrain in North China were less discussed. In addition, the detailed cloud-precipitation physical process that induced the extreme precipitation over Central and North China still remained vague. As a result, the numerical prediction skills of the heavy rainfall in North China were relatively low (Liu et al., 2021). Therefore, the following questions need to be addressed in the future: (1) How to obtain the key signals for the long-lasting extreme precipitation events from the medium-range forecast? (2) What are the quantitative influences of the terrain in western Henan Province on the triggering, development of the conventions and the precipitation? (3) What are the cloud-precipitation physical mechanisms of the extreme hourly precipitation in North China? (4) How to predict the extreme heavy rainfall center by using the high-resolution numerical prediction model?

## AUTHOR CONTRIBUTIONS

**Jianhua Sun:** Conceptualization; data curation; formal analysis; funding acquisition; project administration; supervision; writing – original draft; writing – review and editing. **Shenming Fu:** Data curation; formal analysis; investigation; methodology; software; writing – original draft; writing – review and editing. **Huijie Wang:** Investigation; software; validation; visualization. **Yuanchun Zhang:** Investigation; project administration; validation; visualization. **Yun Chen:** Supervision. **Aifang Su:** Resources. **Yaqiang Wang:** Software; visualization. **Huan Tang:** Resources; software; visualization. **Ruoyun Ma:** Software; visualization.

## ACKNOWLEDGEMENTS

This research was supported by the National Key Research and Development Program of China (Grant 2019YFC1510400), and the National Natural Science Foundation of China (Grant Nos. 42075002, 41975057 and U2142202).

## DATA AVAILABILITY STATEMENT

The daily and hourly precipitation observation at meteorological stations from the China Meteorological Administration are available at http://data.cma.cn/en/?r=data/index&cid=9e5e973ce269a309. The ERA5 reanalysis data is downloaded from https://cds.climate.copernicus.eu/cdsapp#!/dataset/reanalysis-era5-pressure-levels?tab=form.

## ORCID

*Shenming Fu* https://orcid.org/0000-0001-9670-0607
*Yuanchun Zhang* https://orcid.org/0000-0003-3038-9320

## REFERENCES

Bartels, D.L. & Maddox, R.A. (1991) Midlevel cyclonic vortices generated by mesoseale convective systems. *Monthly Weather Review*, 119(1), 104–118. https://doi.org/10.1175/1520-0493(1991)119<0104:MCVGBM>2.0.CO;2

Carissimo, B.C., Pierrehumbert, R.T. & Pham, H.L. (1988) An estimate of mountain drag during ALPEX for comparison with numerical models. *Journal of Atmospheric Sciences*, 45(13), 1949–1960. https://doi.org/10.1175/1520-0469(1988)045<1949:AEOMDD>2.0.CO;2

Davis, C., Atkins, N., Bartels, D., Bosart, L., Coniglio, M., Bryan, G. et al. (2004) The bow echo and mcv experiment: observations and opportunities. *Bulletin of the American Meteorological Society*, 85(8), 1075–1094. https://doi.org/10.1175/BAMS-85-8-1075

Ding, Y., Li, J., Sun, S., Cai, Z.Y., Zhao, S.X. & Tao, S.Y. (1980) The analysis on mesoscale systems producing heavy rainfall in North China (in Chinese with English abstract). *Institute of Atmospheric Physics, Chinese Academy of Sciences*, 9, 1–13.

Ding, Y. (2015) On the study of the unprecedented heavy rainfall in Henan Province during 4–8 august 1975: review and assessment (in Chinese with English abstract). *Acta Meteorologica Sinica*, 73, 411–424.

Draxler, R.R. (1999) *HYSPLIT4 user's guide. NOAA technical memorandum ERL ARL-230*. Silver Spring, MD: Air Resources Laboratory.

Draxler, R.R. & Hess, G.-D. (1998) An overview of the HYSPLIT_4 modeling system of trajectories, dispersion, and deposition. *Australian Meteorological Magazine*, 47(4), 295–308.

Feng, S.-L., Jin, S.-L., Fu, S.-M., Sun, J.-H. & Zhang, Y.-C. (2019) Formation of a kind of heavy-rain-producing mesoscale vortex

1530261x, 0, Downloaded from https://rmets.onlinelibrary.wiley.com/doi/10.1002/asl.1131 by Institution Of Atmospheric Physics, Wiley Online Library on [29/11/2022]. See the Terms and Conditions (https://onlinelibrary.wiley.com/terms-and-conditions) on Wiley Online Library for rules of use; OA articles are governed by the applicable Creative Commons License

around the Sichuan Basin: an along-track vorticity budget analysis. *Atmospheric Science Letters*, 2019, e949.

Fu, S., Sun, J., Luo, Y. & Zhang, Y. (2017) Formation of long-lived summertime mesoscale vortices over central East China: semi-idealized simulations based on a 14-year vortex statistic. *Journal of the Atmospheric Sciences*, 74(12), 3955–3979. doi:10.1175/JAS-D-16-0328.1

Fu, S.-M., Mai, Z., Sun, J.-H., Li, W.-L., Ding, Y. & Wang, Y.-Q. (2019) Impacts of convective activity over the Tibetan plateau on plateau vortex, southwest vortex, and downstream precipitation. *Journal of the Atmospheric Sciences*, 76, 3803–3830.

Fu, S.-M., Zhang, Y.-C., Wang, H.-J., Tang, H., Li, W.-L. & Sun, J.-H. (2022a) On the evolution of a long-lived mesoscale convective vortex that acted as a crucial condition for the extremely strong hourly precipitation in Zhengzhou. *Journal of Geophysical Research – Atmospheres*, 127, e2021JD036233.

Fu, S.-M., Zhang, J.-P., Tang, H., Jiang, L.-Z. & Sun, J.-H. (2020) A new mesoscale-vortex identification metric: restricted vorticity and its application. *Environmental Research Letters.*, 15, 124053. https://doi.org/10.1088/1748-9326/abcac6

Fu, S.-M., Tang, H., Sun, J.-H., Zhao, T.-B. & Li, W.-L. (2022b) Historical rankings and vortices' activities of the extreme Mei-yu seasons: contrast 2020 to previous Mei-yu seasons. *Geophysical Research Letters*, 49, e2021GL096590. https://doi.org/10.1029/2021GL096590

Compilers of Heavy rainfall in North China. (1992) *Heavy rainfall in North China (in Chinese)*. Beijing: China Meteorological Press, p. 182.

Hersbach, H., Bell, B., Berrisford, P., Hirahara, S., Horányi, A., Munoz-Sabater, J. et al. (2020) The ERA5 global reanalysis. *Quarterly Journal of the Royal Meteorological Society*, 146(730), 1999–2049. doi:10.1002/qj.3803

Holton, J.R. (2004) *An introduction to dynamic meteorology*. San Diego: Academic Press, p. 552.

Li, W., Ma, H., Fu, R., Han, H. & Wang, X. (2022) Development and maintenance mechanisms of a longlived mesoscale vortex which governed the earlier stage of the "21.7" Henan torrential rainfall event. *Frontiers in Earth Science*, 10, 909662. https://doi.org/10.3389/feart.2022.909662

Liu, C., Sun, J., Yang, X., Jin, S. & Fu, S. (2021) Evaluation of ECMWF precipitation predictions in China during 2015–18. *Weather and Forecasting*, 36, 1043–1060. https://doi.org/10.1175/WAF-D-20-0143.1

Luo, Y., Wu, M., Ren, F., Li, J. & Wong, W. (2016) Synoptic situations of extreme hourly precipitation over China. *Journal of Climate*, 29(24), 8703–8719. https://doi.org/10.1175/JCLI-D-16-0057.1

Luo, Y., Sun, J., Li, Y., Xia, R., Du, Y., Yang, S. et al. (2020) Science and prediction of heavy rainfall over China: research progress since the reform and opening-up of new China. *Journal of Meteorological Research*, 34(3), 427–459. https://doi.org/10.1007/s13351-020-0006-x

Markowski, P. & Richardson, Y. (2010) *Mesoscale meteorology in midlatitudes*. Hoboken, NJ: Wiley-Blackwell, p. 407.

Raymond, D.J. & Jiang, H. (1990) A theory for long-lived mesoscale convective systems. *Journal of Atmospheric Sciences*, 47(24), 3067–3077. https://doi.org/10.1175/1520-0469(1990)047<3067:ATFLLM>2.0.CO;2

Stein, A.F., Draxler, R.R., Rolph, G.D., Stunder, B.J.B., Cohen, M. D. & Ngan, F. (2015) NOAA's HYSPLIT atmospheric transport and dispersion modeling system. *Bulletin of the American Meteorological Society*, 96(12), 2059–2077. https://doi.org/10.1175/BAMS-D-14-00110.1

Sun, J.H., Wang, H.J., Wei, J. & Qi, L.L. (2016) The sources and transportation of water vapor in persistent heavy rainfall events in the Yangtze-Huaihe River Valley (in Chinese with English abstract). *Acta Meteorologica Sinica*, 74, 542–555.

Sun, J.H., Zhang, X.L., Wei, J. & Zhao, S.X. (2005) A study on severe heavy rainfall in North China during the 1990s (in Chinese with English abstract). *Climatic and Environmental Research*, 10, 492–506.

Sun, J.H., Zhao, S.X., Fu, S.M., Wang, H.J. & Zheng, L.L. (2013) Multi-scale characteristics of record heavy rainfall over Beijing area on July 21, 2012 (in Chinese with English abstract). *Chinese Journal of Atmospheric Sciences*, 37(3), 705–718.

Sun, J.S. (2005) The effects of vertical distribution of the lower level flow on precipitation location. *Plateau Meteorology*, 24(1), 62–69 (in Chinese with English abstract).

Sun, J.S. & Yang, B. (2008) Meso-β scale torrential rain affected by topography and the urban circulation (in Chinese with English abstract). *Chinese Journal of Atmospheric Sciences*, 32(6), 1352–1364.

Tao, S.Y. (1980) *Heavy rainfalls in China (in Chinese)*. Beijing: Science Press, p. 225.

Tutiš, V. & Ivančan-Picek, B. (1991) Pressure drag on the Dinaric Alps during the ALPEX SOP. *Meteorology and Atmospheric Physics*, 47(1), 73–81. https://doi.org/10.1007/BF01025829

Xia, R. & Zhang, D. (2019) An observational analysis of three extreme rainfall episodes of 19–20 July 2016 along the Taihang Mountains in North China. *Monthly Weather Review*, 147(11), 4199–4220. https://doi.org/10.1175/MWR-D-18-0402.1

Yin, J.-F., Gu, H.-D., Liang, X.-D., Yu, M., Sun, J.-S., Xie, Y.-X. et al. (2022) A possible dynamic mechanism for rapid production of the extreme hourly rainfall in Zhengzhou City on 20 July 2021. *Journal of Meteorological Research*, 36, 1–20.

Zhang, H. & Zhai, P. (2011) Temporal and spatial characteristics of extreme hourly precipitation over eastern China in the warm season. *Advances in Atmospheric Sciences*, 28(5), 1177–1183. https://doi.org/10.1007/s00376-011-0020-0

Zhang, Y.-C., Fu, S.-M., Sun, J.-H., Fu, R., Jin, S.-L. & Ji, D.-S. (2019) A 14-year statistics-based semi-idealized modeling study on the formation of a type of heavy rain–producing southwest vortex. *Atmospheric Science Letters*, 2019, e894.

**How to cite this article:** Sun, J., Fu, S., Wang, H., Zhang, Y., Chen, Y., Su, A., Wang, Y., Tang, H., & Ma, R. (2022). Primary characteristics of the extreme heavy rainfall event over Henan in July 2021. *Atmospheric Science Letters*, e1131. https://doi.org/10.1002/asl.1131

1530261x, 0, Downloaded from https://rmets.onlinelibrary.wiley.com/doi/10.1002/asl.1131 by Institution Of Atmospheric Physics, Wiley Online Library on [29/11/2022]. See the Terms and Conditions (https://onlinelibrary.wiley.com/terms-and-conditions) on Wiley Online Library for rules of use; OA articles are governed by the applicable Creative Commons License